applied sciences

MDPI

Article

Comparative Evaluation of Laser System to Conventional Surgical Approaches in Periodontal Healing Using Optical Coherence Tomography

Jun-Hyeong Park [1,†], Keun-Ba-Da Son [2,†], Young-Tak Son [2,3,†], Yong-Gun Kim [1], Sung-Min Hwang [1], Jun-Ho Hwang [4], Jong-Hoon Lee [4], Hyun-Deok Kim [5], Kyu-Bok Lee [6,*] and Jae-Mok Lee [1,*]

[1] Department of Periodontology, School of Dentistry, Kyungpook National University, Daegu 41940, Republic of Korea; bi021499@gmail.com (J.-H.P.); periokyg@knu.ac.kr (Y.-G.K.); lhwangl89@naver.com (S.-M.H.)
[2] Advanced Dental Device Development Institute (A3DI), Kyungpook National University, Daegu 41940, Republic of Korea; oceanson@knu.ac.kr (K.-B.-D.S.); dudxkr741@naver.com (Y.-T.S.)
[3] Department of Dental Science, Graduate School, Kyungpook National University, Daegu 41940, Republic of Korea
[4] Institute of Advanced Convergence Technology, Kyungpook National University, Daegu 41061, Republic of Korea; hjh@iact.or.kr (J.-H.H.); laser@knu.ac.kr (J.-H.L.)
[5] School of Electronics Engineering, Kyungpook National University, Daegu 41566, Republic of Korea; hdkim@knu.ac.kr
[6] Department of Prosthodontics, School of Dentistry, Kyungpook National University, Daegu 41940, Republic of Korea
* Correspondence: kblee@knu.ac.kr (K.-B.L.); leejm@knu.ac.kr (J.-M.L.)
† These authors contributed equally to this work.

Abstract: Background: Optical coherence tomography (OCT) is an emerging, radiation-free diagnostic tool in dentistry, providing high-resolution, real-time imaging of both hard and soft tissues, including periodontal areas, for more accurate postoperative evaluations. This study aims to investigate the efficacy of OCT on periodontal tissues in animals by comparing the healing effects of laser therapy with those of conventional surgical instruments. Methods: Six rabbits underwent periodontal surgery using a laser, scalpel, and punch to perform an apically positioned flap on the mandibular anterior incisors and to create a tongue ulcer on the dorsal surface of the tongue. Visual and OCT evaluations were conducted on days 1, 2, 3, 7, and 14. Results: In periodontal surgery, the laser exhibited slightly faster healing compared to other methods. In tongue ulcer formation, the scalpel and punch groups demonstrated slightly faster healing than that of the laser. However, both methods ultimately showed similar healing outcomes. Conclusions: In the dental field, OCT is emerging as a valuable tool for assessing healing, including early stages of healing, in periodontal therapy.

Keywords: dental laser system; optical coherence tomography; periodontal healing

Citation: Park, J.-H.; Son, K.-B.-D.; Son, Y.-T.; Kim, Y.-G.; Hwang, S.-M.; Hwang, J.-H.; Lee, J.-H.; Kim, H.-D.; Lee, K.-B.; Lee, J.-M. Comparative Evaluation of Laser System to Conventional Surgical Approaches in Periodontal Healing Using Optical Coherence Tomography. *Appl. Sci.* **2024**, *14*, 8854. https://doi.org/10.3390/app14198854

Academic Editor: Bruno Chrcanovic

Received: 28 August 2024
Revised: 25 September 2024
Accepted: 27 September 2024
Published: 2 October 2024

1. Introduction

Several periodontal surgical methods have been proposed to treat periodontitis, but further evaluation of these treatments remains crucial. Postoperative evaluations typically rely on the symptoms of the patient, radiographic imaging, and clinical examinations. However, superficial assessments and indirect radiographic evaluations make it challenging to accurately assess changes in soft tissue healing. Histological evaluation is currently the most accurate method for assessing soft tissue healing patterns [1,2]. However, performing histological evaluation on all patients is impractical, highlighting the need for a more convenient method.

The use of laser systems in periodontal treatment is becoming more common. Various positive results indicate that lasers can facilitate easier and faster removal of granulation

tissue compared to traditional methods using a blade [3,4]. Lasers are also effective in treating peri-implantitis [5,6], making this an emerging field of research. Evaluating the healing outcomes of periodontal surgery with laser systems is crucial for their effectiveness.

Optical coherence tomography (OCT) is a valuable imaging device that provides optical cross-sectional images of biological tissues. Initially used in ophthalmology to examine microstructures, including the retina [7], OCT has also been applied to study skin regeneration and re-epithelialization [8,9]. Ongoing efforts were observed to extend its use to various other fields [10,11]. In dentistry, OCT is now used to measure hard tissues such as dental caries, cracks, and calculus [12–15]. Efforts are being made to apply OCT in periodontal areas, including gingival sulcus, tissue thickness, and biological width [16–20]. Based on these efforts, OCT is also being introduced as a diagnostic tool in dentistry, emerging as a highly useful evaluation method. This imaging system uses near-infrared laser light, eliminating the risk of radiation exposure. Furthermore, this modality can create high-resolution, real-time cross-sectional images chair-side. Therefore, OCT is proposed as a tool that can perform postoperative evaluations more simply and accurately than histological and radiographic methods. To properly evaluate periodontal treatments, supplementary examination methods are needed alongside radiographic and clinical evaluations.

Therefore, with the hypothesis that using OCT to assess periodontal tissue provides a more direct indication of healing in real time, this study aims to investigate the effectiveness of OCT by comparing the healing patterns of laser treatment and general surgical tools in the periodontal tissue of animal models.

2. Materials and Methods

2.1. Materials

A laser device (Kyungpook National University, SaeshinJeongmil, Daegu, Republic of Korea), scalpel (#15 blade, Carl Martin, Solingen, Nordrhein-Westfalen, Germany), and tissue punch (Disposable Biopsy dermal punches, KAI Medical, Honolulu, HI, USA) were sealed in 15 mL tubes and stored in a refrigerator after UV disinfection (Figure 1).

(**a**) (**b**) (**c**)

Figure 1. (**a**) Laser device, (**b**) Scalpel, and (**c**) Tissue punch.

The optical coherence tomography (OCT) equipment was brought into the operating room after alcohol disinfection and retained until the end of the experiment (Figure 2).

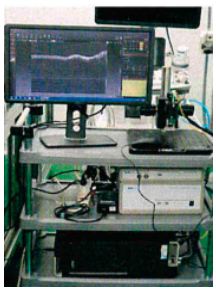

Figure 2. OCT equipment.

The animals used for the experiment were rabbits of the New Zealand White (NZW) strain and consisted of six males over 3 kg. The animals were acclimatized for at least 7 days after acquisition, observed for general symptoms, and confirmed to be healthy before use. All experiments were conducted at the K-MEDI Hub Preclinic Center by the

Kyungpook National University Industry-Academic Cooperation Foundation. The experimental procedures were approved by the Institutional Animal Care and Use Committee (Approval number: KMEDI-22090202-00).

2.2. Methods

2.2.1. Apically Positioned Flap

The experiments were conducted using six rabbits (numbers #1101 to #1106). After measuring their body weight, anesthesia was administered with Ketamine (35 mg/kg, IM)/Rompun (5 mg/kg/IM). Furthermore, an apically positioned flap (APF) was created on the left side of the lower anterior teeth of the rabbit using a scalpel and on the right side using a laser in a contralateral manner (Emission Mode: CW (Continuous Wave) Pulse 10 Hz, Pulse 100 Hz, Pulse 8 kHz). A scalloping incision was made from the gingival margin to the alveolar crest, and a vertical incision was made to the mucogingival junction from the gingival margin at the line angle of the lower anterior teeth. Subsequently, a partial-thickness flap was elevated using a periosteal elevator for blunt dissection. Once the flap was sufficiently mobile to be moved apically, it was sutured and secured to the periosteum. After suturing, meloxicam (0.2 mg/kg, SC) and gentamicin (5 mg/kg, SC) were administered for 3 days (Figure 3).

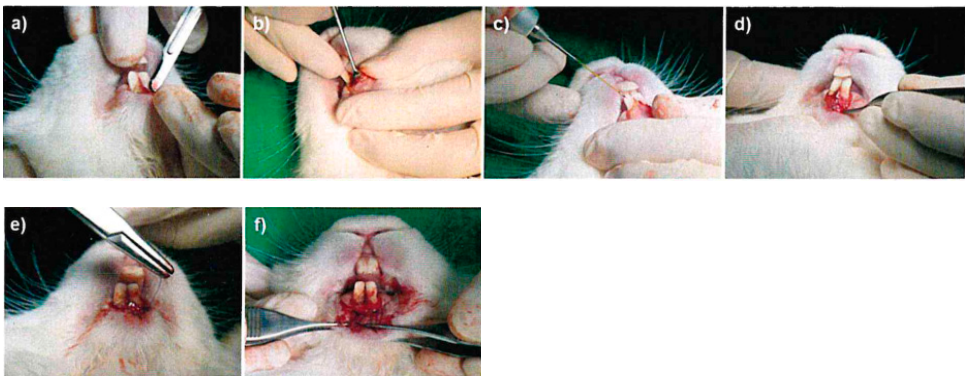

Figure 3. (**a**,**b**,**e**) Apically positioned flap using a scalpel and (**c**,**d**,**f**) laser.

2.2.2. Tongue Ulcer

The same rabbits were used for additional experiments. After measuring their body weights, anesthesia was administered using Ketamine (35 mg/kg, IM)/Rompun (5 mg/kg/IM). Two ulcers were created on the dorsal surface of the tongue using a tissue punch and laser with 6 mm diameter and 1 mm depth. Without additional sutures, meloxicam (0.2 mg/kg, SC) and gentamicin (5 mg/kg, SC) were administered for 3 days (Figure 4).

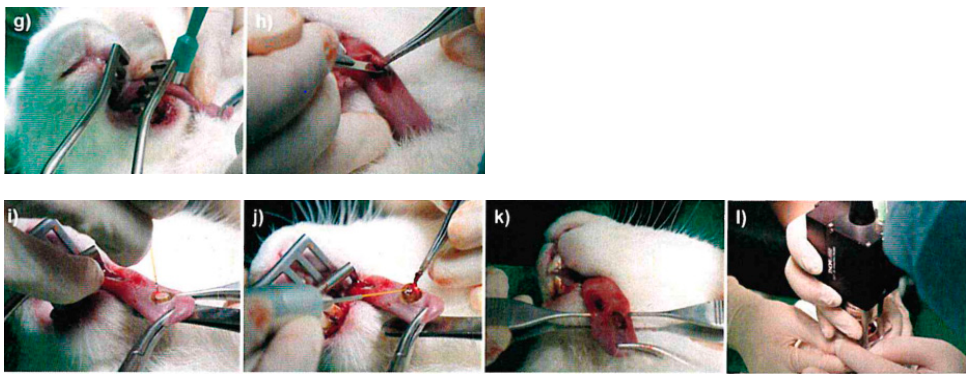

Figure 4. (**g**,**h**) Tongue ulcer formation using tissue punch and (**i**,**j**) laser. (**k**) Two ulcer formations and (**l**) OCT scanning.

2.3. Evaluation

Daily observations were conducted to monitor specific symptoms and check for mortality, with any abnormalities recorded separately. Photographs of the application area were taken and documented on days 1, 2, 3, 7, and 14 after the procedure. Two experienced practitioners used the Early Healing Score (EHS) to visually assess the initial healing process of the APF (Figure 5) [21,22]. The EHS consists of three parameters: clinical signs of re-epithelization (CSR), clinical signs of hemostasis (CSH), and clinical signs of inflammation (CSI). For tongue ulcers, the Healing index of Landry, Turnbull, and Howley (LTH) was used for assessment [23]. Moreover, OCT scans were performed on days 0, 1, 2, 3, 7, and 14 after the procedure. The OCT images were captured using Swept Source-OCT equipment (Thorlabs, Newton, NJ, USA) with a central wavelength of 1300 nm, A-scan Rate of 100 kHz, depth resolution of 7 μm, and lateral resolution of 14 μm. The region of interest (ROI) was 8 mm × 8 mm.

Parameter	Description	Points
CSR	Merged incision margins	6
	Incision margins in contact	3
	Visible distance between incision margins	0
CSH	Absence of fibrin on the incision margins	2
	Presence of fibrin on the incision margins	1
	Bleeding at the incision margins	0
CSI	Absence of redness along the incision length	2
	Redness involving <50% of the incision length	1
	Redness involving >50% of the incision length and/or pronounced swelling	0
Maximum total score: 10		

EHS: Early Wound Healing Score, CSR: clinical signs of re-epithelialization, CSH: clinical signs of haemostasis, CSI: clinical signs of inflammation.

Figure 5. EHS used for the assessments.

2.4. Statistical Analysis

All data were analyzed using statistical software (SPSS ver. 25.0; IBM, Chicago, IL, USA) ($\alpha = 0.05$). To analyze the agreement between the two raters, intraclass correlation coefficient (ICC) values were calculated, and Cohen's Kappa test was used to assess the reliability. The normal distribution of the data was investigated through the Shapiro–Wilk test. As the data were normal, the differences between the groups were analyzed using a paired *t*-test and a one-way ANOVA test.

3. Results

3.1. Visual Evaluation

One rabbit died on the 8th day after surgery. On day 1 after the APF procedure, the left and right sides showed clear scarring, with no differences observed between the laser and other surgical tools. Starting at day 2, all scalpel-treated rabbits exhibited relatively rapid healing. By the 7th day, the scalpel-treated sites were mostly healed. The laser-treated ulcerated area achieved hemostasis immediately after application; however, the wound remained significantly larger than the tissue punch-treated sites. On the 7th day of ulcer formation, the tissue punch-treated sites were mostly healed, while the laser-treated site had a large scar. On the 14th day after ulcer formation, partial healing was observed at the laser-treated sites, but scars remained (Figure 6).

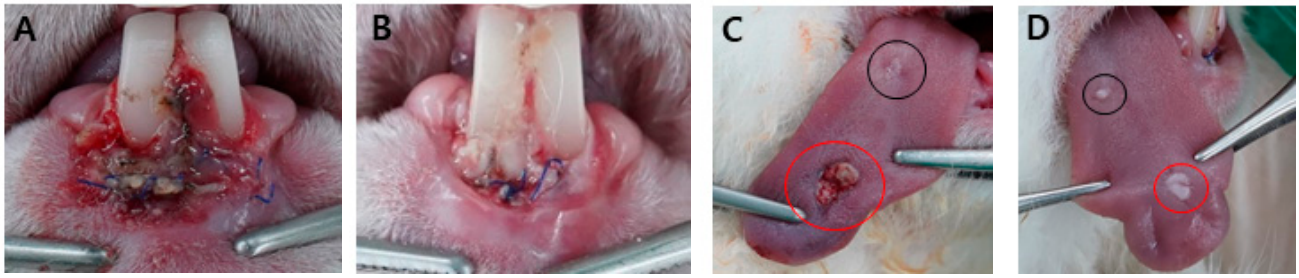

Figure 6. (**A**) On day 1 after APF, carbonization was observed through laser treatment under the right incisor. (**B**) On day 7, scalpel-applied sites were mostly healed. (**C**) At day 7, a difference in healing speed was observed between the laser and punch treatments for tongue ulcers (black circle: punch-treated, red circle: laser-treated) (**D**) On day 14, punch-treated sites were healed with small scars, whereas laser-treated sites showed large scars (black circle: punch-treated, red circle: laser-treated).

3.2. EHS and LTH Score

First, the intraclass correlation coefficient (ICC) values were evaluated to analyze the agreement of results between two evaluators using Cohen's Kappa test [24,25]. The ICC value was 0.936, indicating excellent agreement between the evaluators ($p < 0.001$). Regarding the difference in the initial healing response of the two methods for APF, the laser showed a higher healing score than that of the scalpel in the first 3 days, with statistical significance (†). However, after 7 and 14 days, no significant differences were observed between the two methods. Additionally, no statistical difference was observed in the overall effectiveness of the two methods (††), while statistical significance was found in healing changes over time within both methods (†††) (Table 1).

Table 1. Comparison of early wound healing scores between two treatment methods for apically positioned flap operation.

Day	Treatment	Mean	SD	95% Confidence Interval		Minimum	Maximum	t	p †	p ††
				Lower	Upper					
D1	Laser	4.75	1.21	3.9778	5.5222	3	6	2.932	0.014 *	0.178
	Scalpel	3.08	1.83	1.9194	4.2473	1	7			
D2	Laser	6.25	1.54	5.2685	7.2315	4	9	3.026	0.012 *	
	Scalpel	5.16	1.46	4.2347	6.0986	3	9			
D3	Laser	7.91	1.72	6.8176	9.0158	4	9	2.31	0.041 *	
	Scalpel	6.75	2.26	5.3132	8.1868	3	10			
D7	Laser	8.33	2.05	7.0247	9.642	4	10	2	0.071	
	Scalpel	7.66	1.87	6.4754	8.8579	4	10			
D14	Laser	9	1.56	7.8816	10.1184	5	10	−1.152	0.279	
	Scalpel	9.3	1.56	8.179	10.421	5	10			
p †††	Laser					<0.001 *				
	Scalpel					<0.001 *				

* Significant difference between two treatment methods determined by a paired t-test, $p < 0.05$. † Indicates statistical significance using a paired t-test comparing the two treatment methods on specific days. †† Indicates statistical significance using repeated measures ANOVA evaluating the overall effect of the two treatment methods across the entire period. ††† Indicates statistical significance using repeated measures ANOVA analyzing changes over time within each treatment method.

For tongue ulcer operation, no significant difference was observed between the methods during the first 2 days. However, from day 3 onward, a significant difference emerged

between the methods (†). Overall, the healing response with the punch method was significantly better than that of the laser method (††). Additionally, significant differences were found in healing changes over time within both methods (†††) (Table 2).

Table 2. Comparison of early wound healing scores between two treatment methods for tongue ulcer operation.

Day	Treatment	Mean	SD	95% Confidence Interval		Minimum	Maximum	t	p †	p ††
				Lower	Upper					
D1	Laser	2.08	0.28	1.8999	2.2667	**2**	**3**	−0.432	0.674	0.006 * (Laser < Punch)
	Punch	2.16	0.57	1.7998	2.5335	1	3			
D2	Laser	2.58	0.66	2.1586	3.0081	2	4	−0.321	0.754	
	Punch	2.66	0.88	2.1027	3.2306	1	4			
D3	Laser	2.83	0.57	2.4665	3.2002	2	4	−2.569	0.026 *	
	Punch	3.33	0.65	2.9195	3.7472	2	4			
D7	Laser	3.25	0.45	2.9626	3.5374	3	4	−7.091	<0.001 *	
	Punch	4.58	0.51	4.2562	4.9105	4	5			
D14	Laser	3.7	0.48	3.3544	4.0456	3	4	−8.315	<0.001 *	
	Punch	5	0	5	5	5	5			
p †††	Laser					<0.001 *				
	Punch					<0.001 *				

* Significant difference between two treatment methods determined by a paired t-test, $p < 0.05$. † Indicates statistical significance using a paired t-test to compare the two treatment methods on specific days. †† Indicates statistical significance using repeated measures ANOVA to evaluate the overall effect of the two treatment methods across the entire period. ††† Indicates statistical significance using repeated measures ANOVA to analyze changes over time within each treatment method.

3.3. OCT Analysis

3.3.1. Apically Positioned Flap

Three observation areas were selected and monitored: the area of the vertical incision, the open wound area above the sutured line after the APF, and the junction area of the flap after the APF procedure (Figure 7).

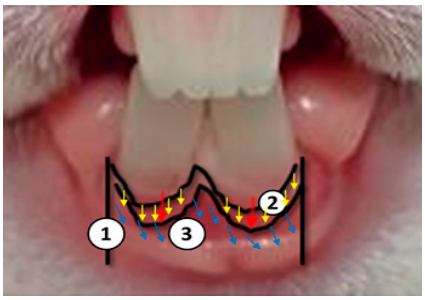

Figure 7. Components of OCT analysis include (1) the area of the vertical incision, (2) the area of the open wound above the sutured line (red arrows) after the apically positioned flap (yellow arrows), and (3) the area of the flap junction after the apically positioned flap (blue arrows).

In OCT images, periodontal structures were clearly depicted. The oral epithelium emerged darker than the underlying connective tissue owing to lower scattering and signal intensity. The connective tissue is characterized by its brighter structure and high signal intensity. Similarly, the alveolar bone appeared darker owing to its lower signal intensity.

Laser

On days 0 and 1 after surgery, inflammatory tissues were observed. These tissues could be distinguished by the absence of the normal internal structures found in healthy gingival tissue. By days 2 and 3, the gingival tissue began to recover, showing the formation of normal tissue structures and regaining its thickness. By day 7, mild inflammation tissues were observed. By day 14, the gingival tissue showed almost complete recovery (Figure 8).

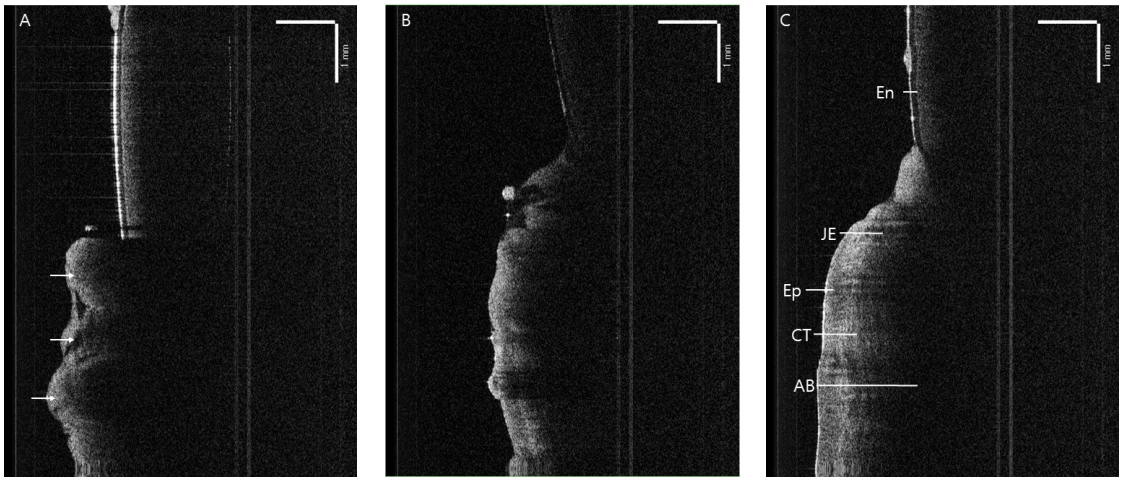

Figure 8. (**A**) OCT image on day 1 after apically positioned flap with laser. Inflammatory tissues were dominant at the gingival level below the teeth (white arrows). (**B**) OCT image on day 3 shows the inflammatory response and recovery phase. (**C**) OCT image on day 14 shows the normal gingival tissue structure [19]. (En: Enamel, JE: Junctional epithelium, Ep: Gingival epithelium, CT: Connective tissue, AB: Alveolar bone).

Scalpel

On days 0 and 1, inflammatory tissues were present; however, the original structure showed minimal abnormalities. By days 2 and 3, gingival recovery was progressing rapidly. By days 7 and 14, the healing of the gingival tissue was comparable to that of the laser-treated models (Figure 9).

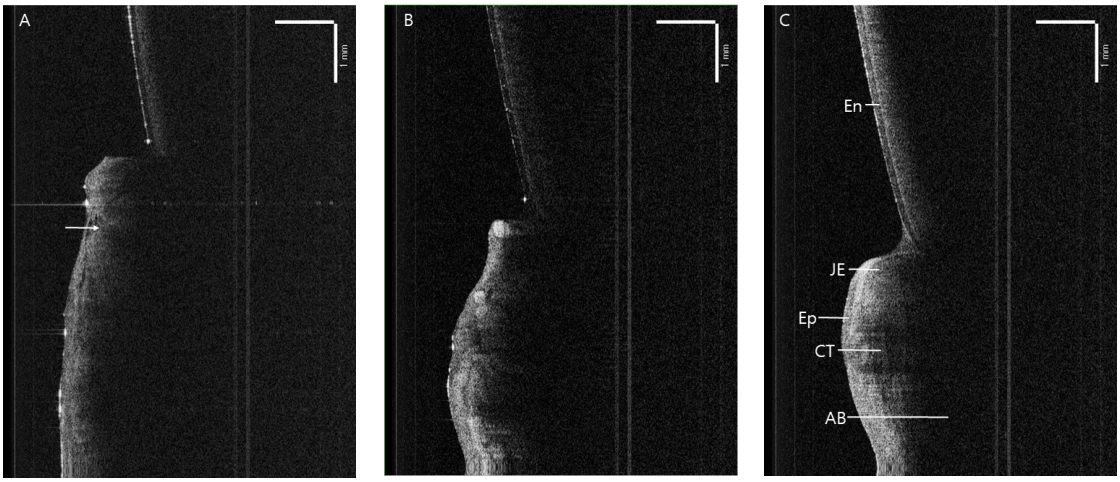

Figure 9. (**A**) OCT image on day 1 after apically positioned flap with a scalpel. Inflammatory tissues were observed in the gingival area while maintaining its shape (white arrow). (**B**) OCT image taken on day 3 shows an inflammatory response, with the recovery phase beginning rapidly. (**C**) OCT image taken on day 14 reveals the restoration of normal gingival tissue structure (En: Enamel, JE: Junctional epithelium, Ep: Gingival epithelium, CT: Connective tissue, AB: Alveolar bone).

3.3.2. Tongue Ulcer

Laser

On days 0 and 1 after ulcer formation, large surgical defects with reduced soft tissue thickness were observed.

By days 2 and 3, inflammation was present, along with rapid healing. By days 7 and 14, the tissue showed nearly complete healing (Figure 10).

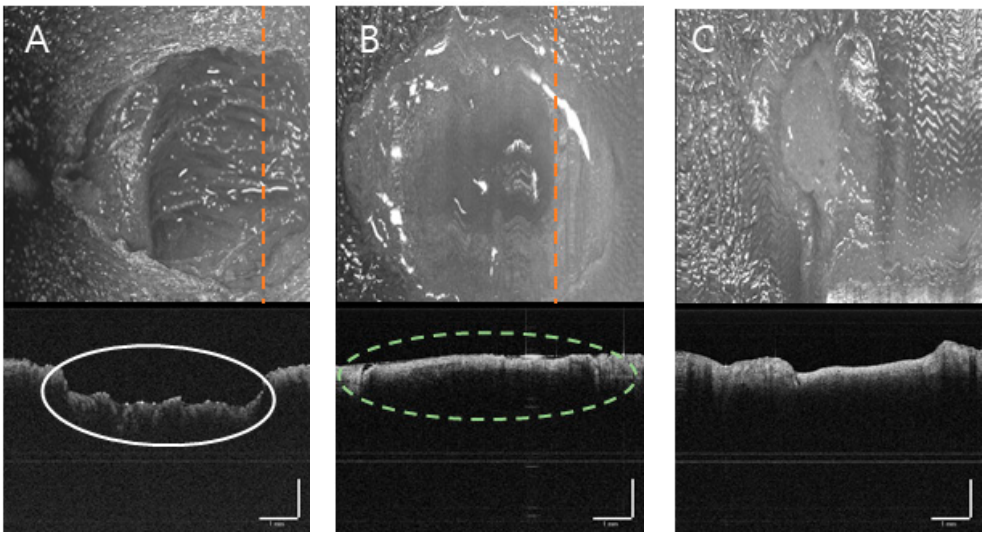

Figure 10. OCT image with en face view of the ulcer by laser (orange line: the side where the OCT image acquired): (**A**) On day 0, a few amounts of blood with ulcerative wounds were found (white circle). (**B**) On day 3, rapid healing and tissue volume recovery are observed (green circle). (**C**) By day 14, the tissue shows nearly complete healing with a visible scar.

Tissue Punch

On days 0 and 1 after ulcer formation, blood was present in the ulcerative wound, resulting in a shallower penetration depth compared to those in other areas. On days 2 and 3, minimal blood remained, and the healing phase progressed rapidly. By days 7 and 14, the wound had completely healed (Figure 11).

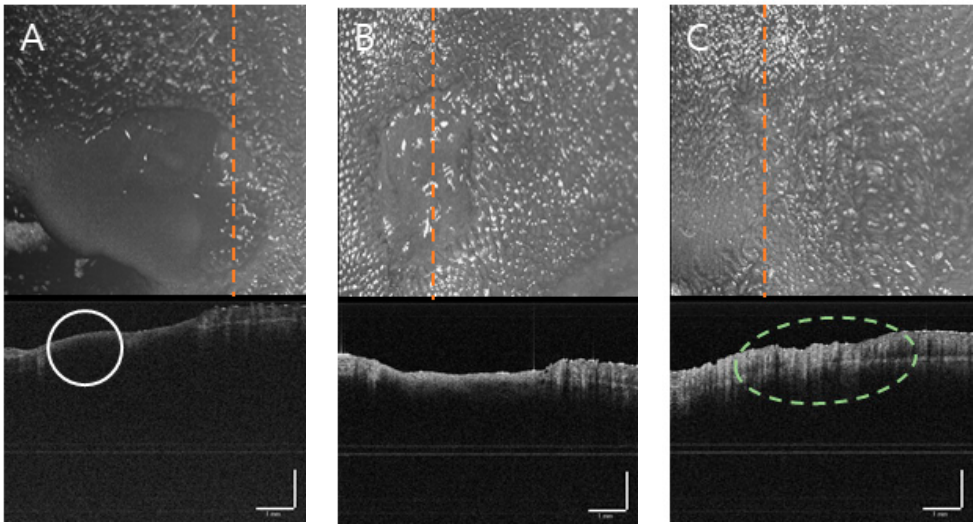

Figure 11. OCT image with en face view of the ulcer by scalpel (orange line: the side where the OCT image acquired): (**A**) On day 0, blood was present at the ulcerative wound (white circle). (**B**) By day 2, rapid healing was observed. (**C**) By day 14, the wound had completely healed without any scarring (green circle).

4. Discussion

Based on visual assessments, including EHS and LTH scores, rapid healing was observed in all the groups. The conventional surgical tool group exhibited a more aesthetic healing pattern and was slightly faster than that of the laser group. However, statistical analysis revealed that while the laser group demonstrated good initial hemostasis in periodontal surgical procedures, it also resulted in carbonization and unaesthetic scarring, particularly in the tongue ulcer sites. This may be owing to the laser intensity or other conditions not being perfectly suited to the animal or thin biotype. Additionally, the heat generated during the procedure may have deformed the surrounding tissue, affecting the healing rate [26–28]. In periodontal surgery and tongue ulcer formation, differences in healing patterns were observed owing to variations in laser intensity and application time, which affected different tissue depths.

Histological observation is generally the standard method for observing and evaluating healing patterns in dental research [29]. However, collecting and storing samples is technically challenging and time-consuming. Additionally, sample deformation and size limitations can lead to inaccurate evaluations, as they do not allow for the assessment of the entire soft tissues. Moreover, radiographical evaluation, which is commonly used in clinical practice, has limitations, including difficulty in observing soft tissue, exposure to radiation, and variability in results.

OCT, originally used for ophthalmological and dermatological evaluations, is now emerging as a valuable tool in dental field applications. Beyond assessing hard tissues, OCT is increasingly being used to evaluate soft tissues, including biologic width or wound epithelization. In periodontal treatments, evaluating the structure of periodontal tissue is crucial. Factors such as gingival contour and thickness, gingival and sulcular epithelium, free and attached gingiva, inner connective tissue attachments, and alveolar bone should be assessed before any treatment [16–18]. Unlike histological and radiographical methods, OCT has the advantage of using only infrared lights, which prevents data distortion and allows for comprehensive observation of tissue changes. High-resolution OCT imaging enables detailed assessment of initial conditions, presence of inflammation, lesion progression, healing extent, and long-term follow-up.

Controlling inflammation is crucial for evaluating the outcome of periodontal therapy. Conventional methods for detecting inflammation include visual assessments of redness, edema, and suppuration, bleeding on probing, calculus detection with exploratory devices, and radiographs [30]. However, visual and manual assessments are subjective and limited in their ability to detect detailed changes. Furthermore, radiographic evaluation focuses on detecting bone loss rather than assessing soft tissue, making it challenging to evaluate early inflammation or healing. This study demonstrated changes in the extent of inflammation during the early healing period. In APF cases, both laser-treated and scalpel-treated groups showed an immediate increase in inflammatory tissues lacking normal basement structure. By day 3, the scalpel-treated group exhibited significant inflammation resolution and restoration of normal tissue structure. In the laser-treated groups, remnants of inflammatory tissues were still present on days 3 and 7 in some cases; however, by day 14, healing occurred to a similar extent as in the scalpel-treated groups, although at a faster rate. In the tongue ulcer cases, both laser-treated and punch-treated groups exhibited bleeding in response to ulcer formation. However, the laser-treated groups experienced less bleeding, indicating the hemostasis ability of the laser. By day 7, the punch-treated groups showed significant healing with small scars, whereas the laser-treated groups showed slower healing and larger scars. Based on these results, conventional surgical tools promote a faster healing process compared to laser treatment. Moreover, laser treatment can cause large scars, likely owing to carbonization, although its early hemostatic ability is also related to this process. Additionally, real-time cross-sectional images of the OCT enable the estimation of inflammatory conditions at each stage of healing.

Additionally, gingival thickness is also assessed in the periodontal area. At inflammation sites, the immune response increases blood flow with angiogenesis [31,32], leading

to increased volume, structural changes, and altered texture [33]. Another challenge is recognizing these changes and determining in real time whether they are resolving. In this study, all the groups showed recovery of gingival thickness to normal structure during the early healing period. Initially, volume defects with rough texture indicated abnormalities. In APF cases, significant volume recovery was observed on day 7 in the scalpel-treated groups, while the laser-treated groups showed similar recovery by day 14. In tongue ulcer cases, both groups exhibited significant volume recovery by day 7. However, a reduction in inflamed gingival thickness was discovered in all the groups across both types of cases. Variations in gingival thickness should be considered as an important factor in early healing evaluation [34–36].

Gingival thickness is crucial not only for healing but also for aesthetic periodontal treatments, such as gingival augmentation and root flap surgery. A three-dimensional assessment of the gingival phenotype is essential in these contexts [37]. To achieve predictable outcomes, differentiating between the epithelial and connective tissue layers and accurately measuring their thickness is necessary. Additionally, bleeding control at the donor site can be improved by identifying the locations of palatal vessels.

Observing blood vessels around periodontal tissues is also important. When the inflammatory-immune system activates, one of the most noticeable phenomena is angiogenesis, which can influence the healing process. Blood vessels are typically distinguished from connective tissue by their round or oval shape and lower signal intensity [20]. However, more advanced techniques are available to verify this component, such as OCT with functional angiography (OCT-A) [38,39]. OCT-A can quantify vessel density and the number of blood vessels, aiding in the assessment of inflammation resolution. Additionally, as previously mentioned, it can be particularly useful in delicate surgeries with bleeding risks by visualizing blood vessels.

As mentioned above, the use of OCT is a simple and harmless way to observe the presence of inflammation, soft tissue thickness, and vascularization during the early healing process of periodontal tissue. However, OCT also has limitations that need to be addressed. OCT images became unclear beyond an approximate depth of 1.5 mm [20]. For biological depth measurements, OCT images were approximately 0.41 mm shallower than those obtained from histological calculations [40]. Additionally, the OCT system is less effective at detecting the sulcus anatomy within the furcation, likely owing to its limited penetration depth. To overcome these obstacles, increasing the center wavelength can enhance penetration depth [41]. However, this approach may decrease the resolution of OCT images, necessitating further developments to balance both the imaging depth and quality.

5. Conclusions

OCT is increasingly being adopted in the dental field as a safe, high-resolution, fast, and accessible evaluation tool for periodontal conditions. It offers a simple but precise method for assessing healing and it is expected to become even more valuable as it advances to address its current limitations.

Author Contributions: Conceptualization, K.-B.-D.S., Y.-T.S. and J.-M.L.; Formal analysis, Y.-G.K.; Investigation, J.-H.P., K.-B.-D.S. and Y.-T.S.; Resources, J.-H.H., J.-H.L. and H.-D.K.; Data curation, J.-H.P.; Writing—original draft, J.-H.P.; Writing—review & editing, S.-M.H. and J.-M.L.; Supervision, K.-B.L.; Project administration, J.-M.L. All authors have read and agreed to the published version of the manuscript.

Funding: This work was supported by the National Research Foundation of Korea (NRF) grant funded by the Korean government (MSIT) [grant no. 2022R1C1C2007040], the Korea Institute for Advancement of Technology (KIAT) grant funded by the Ministry of Trade, Industry, and Energy (MOTIE) (P0017662), and the National Research Foundation of Korea (NRF) grant funded by the Ministry of Education (MOE) (2022RIS-006), Republic of Korea.

Institutional Review Board Statement: The research protocol of this study was reviewed and approved by the Institutional Animal Care and Use Committee (Approval number: KMEDI-22090202-00).

Informed Consent Statement: Not applicable.

Data Availability Statement: The raw data supporting the conclusions of this article will be made available by the authors on request.

Conflicts of Interest: The authors declare no conflicts of interest.

References

1. Pilloni, A.; Marini, L.; Gagliano, N.; Canciani, E.; Dellavia, C.; Cornaghi, L.B.; Costa, E.; Rojas, M.A. Clinical, histological, immunohistochemical, and biomolecular analysis of hyaluronic acid in early wound healing of human gingival tissues: A randomized, split-mouth trial. *J. Periodontol.* **2023**, *94*, 868–881. [CrossRef] [PubMed]
2. Yoshino, T.; Aoki, A.; Oda, S.; Takasaki, A.A.; Mizutani, K.; Sasaki, K.M.; Kinoshita, A.; Watanabe, H.; Ishikawa, I.; Izumi, Y. Long-Term Histologic Analysis of Bone Tissue Alteration and Healing Following Er: YAG Laser Irradiation Compared to Electrosurgery. *J. Periodontol.* **2009**, *80*, 82–92. [CrossRef]
3. Haytac, M.C.; Ozcelik, O. Evaluation of Patient Perceptions After Frenectomy Operations: A Comparison of Carbon Dioxide Laser and Scalpel Techniques. *J. Periodontol.* **2006**, *77*, 1815–1819. [CrossRef] [PubMed]
4. Cobb, C.M. Lasers in Periodontics: A Review of the Literature. *J. Periodontol.* **2006**, *77*, 545–564. [CrossRef] [PubMed]
5. Behdin, S.; Monje, A.; Lin, G.-H.; Edwards, B.; Othman, A.; Wang, H.-L. Effectiveness of Laser Application for Periodontal Surgical Therapy: Systematic Review and Meta-Analysis. *J. Periodontol.* **2015**, *86*, 1352–1363. [CrossRef] [PubMed]
6. Kotsakis, G.A.; Konstantinidis, I.; Karoussis, I.K.; Ma, X.; Chu, H. Systematic Review and Meta-Analysis of the Effect of Various Laser Wavelengths in the Treatment of Peri-Implantitis. *J. Periodontol.* **2014**, *85*, 1203–1213. [CrossRef] [PubMed]
7. Sakata, L.M.; Deleon-Ortega, J.; Sakata, V.; Girkin, C.A. Optical coherence tomography of the retina and optic nerve—A review. *Clin. Exp. Ophthalmol.* **2009**, *37*, 90–99. [CrossRef]
8. Glinos, G.D.; Verne, S.H.; Aldahan, A.S.; Liang, L.; Nouri, K.; Elliot, S.; Glassberg, M.; Cabrera DeBuc, D.; Koru-Sengul, T.; Tomic-Canic, M.; et al. Optical coherence tomography for assessment of epithelialization in a human ex vivo wound model. *Wound Repair. Regen.* **2017**, *6*, 1017–1026. [CrossRef]
9. Kuck, M.; Strese, H.; Alawi, S.A.; Meinke, M.C.; Fluhr, J.W.; Burbach, G.J.; Krah, M.; Sterry, M.; Lademann, K. Evaluation of optical coherence tomography as a non-invasive diagnostic tool in cutaneous wound healing. *Skin. Res. Technol.* **2014**, *20*, 1–7. [CrossRef]
10. Poneros, J.M.; Brand, S.; Bouma, B.E.; Tearney, G.J.; Compton, C.C.; Nishioka, N.S. Diagnosis of specialized intestinal metaplasia by optical coherence tomography. *Gastroenterology* **2001**, *120*, 7–12. [CrossRef] [PubMed]
11. Evans, J.A.; Poneros, J.M.; Bouma, B.E.; Bressner, J.; Halpern, E.F.; Shishkov, M.; Lauwers, G.Y.; Kenudson, M.M.; Nishioka, N.S.; Tearney, G.J. Optical coherence tomography to identify intramucosal carcinoma and high-grade dysplasia in Barrett's esophagus. *Clin. Gastroenterol. Hepatol.* **2006**, *4*, 38–43. [CrossRef]
12. Feldchtein, F.; Gelikonov, V.; Iksanov, R.; Kuranov, R.V.; Sergeev, A.M.; Gladkova, N.D.; Ourutina, M.N.; Warren, J.A.; Reitze, D.H. In vivo OCT imaging of hard and soft tissue of the oral cavity. *Opt. Express.* **1998**, *3*, 239–250. [CrossRef] [PubMed]
13. Imai, K.; Shimada, Y.; Sadr, A.; Sumi, Y.; Tagami, J. Noninvasive cross-sectional visualization of enamel cracks by optical coherence tomography in vitro. *J. Endod.* **2012**, *38*, 1269–1274. [CrossRef] [PubMed]
14. Hsieh, Y.S.; Ho, Y.C.; Lee, S.Y.; Lu, C.W.; Jiang, C.P.; Chuang, C.C. Subgingival calculus imaging based on swept-source optical coherence tomography. *J. Biomed. Opt.* **2011**, *16*, 07–09. [CrossRef] [PubMed]
15. Shimada, Y.; Sadr, A.; Sumi, Y.; Tagami, J. Application of Optical Coherence Tomography (OCT) for Diagnosis of Caries, Cracks, and Defects of Restorations. *Curr. Oral. Health Rep.* **2015**, *2*, 73–80. [CrossRef]
16. Mota, C.C.; Fernandes, L.O.; Cimoes, R.; Gomes, A.S. Non-invasive periodontal probing through Fourier-domain optical coherence tomography. *J. Periodontol.* **2015**, *86*, 1087–1109. [CrossRef] [PubMed]
17. Fernandes, L.O.; Mota, C.C.; de Melo, L.S.; da Costa Soares, M.U.; da Silva Feitosa, D.; Gomes, A.S. In vivo assessment of periodontal structures and measurement of gingival sulcus with Optical Coherence Tomography: A pilot study. *J. Biophotonics* **2016**, *10*, 862–869. [CrossRef] [PubMed]
18. Agrawal, P.; Sanikop, S.; Patil, S. New developments in tools for periodontal diagnosis. *Int. Dent. J.* **2012**, *62*, 57–64. [CrossRef] [PubMed]
19. Egreja, A.M.C.; Kahn, S.; Barceleiro, M.; Bittencourt, S. Relationship between the width of the zone of keratinized tissue and thickness of gingival tissue in the anterior maxilla. *Int. J. Periodontics Restor. Dent.* **2012**, *32*, 573–579.
20. Kakizaki, S.; Aoki, A.; Tsubokawa, M.; Lin, T.; Mizutani, K.; Koshy, G.; Sadr, A.; Oda, S.; Sumi, Y.; Izumi, Y. Observation and determination of periodontal tissue profile using optical coherence tomography. *J. Periodontal Res.* **2018**, *53*, 188–199. [CrossRef] [PubMed]
21. Marini, L.; Rojas, M.A.; Sahrmann, P.; Aghazada, R.; Pilloni, A. Early Wound Healing Score: A system to evaluate the early healing of periodontal soft tissue wounds. *J. Periodontal Implant. Sci.* **2018**, *48*, 274–283. [CrossRef]
22. Marini, L.; Sahrmann, P.; Rojas, M.A.; Cavalcanti, C.; Pompa, G.; Papi, P.; Pilloni, A. Early Wound Healing Score (EHS): An Intra- and Inter-Examiner Reliability Study. *Dent. J.* **2019**, *7*, 86. [CrossRef] [PubMed]
23. Landry, R.G.; Turnbull, R.S.; Howley, T. Effectiveness of benzydamyne HCl in the treatment of periodontal post-surgical patients. *Res. Clin. Forums* **1988**, *10*, 105–118.

24. Cicchetti, D.V. Guidelines, criteria, and rules of thumb for evaluating normed and standardized assessment instruments in psychology. *Psychol. Assess.* **1994**, *6*, 284–290. [CrossRef]
25. Koo, T.K.; Li, M.Y. A Guideline of Selecting and Reporting Intraclass Correlation Coefficients for Reliability Research. *J. Chiropr. Med.* **2016**, *15*, 155–163. [CrossRef]
26. Centty, I.G.; Blank, L.W.; Levy, B.A.; Romberg, E.; Barnes, D.M. Carbon dioxide laser for de-epithelialization of periodontal flaps. *J. Periodontol.* **1997**, *68*, 763–769. [CrossRef] [PubMed]
27. Kara, C.; Demir, T.; Ozbek, E. Evaluation of low-level laser therapy in rabbit oral mucosa after soft tissue graft application: A pilot study. *J. Cosmet. Laser Ther.* **2013**, *15*, 326–329. [CrossRef] [PubMed]
28. Amorim, J.C.; de Sousa, G.R.; de Barros Silveira, L.; Prates, R.A.; Pinotti, M.; Ribeiro, M.S. Clinical study of the gingiva healing after gingivectomy and low-level laser therapy. *Photomed. Laser Surg.* **2006**, *24*, 588–594. [CrossRef]
29. Lins, R.D.A.U.; Figueiredo, C.R.L.V.; Queiroz, L.M.G.; Silveira, E.J.D.d.; Godoy, C.P.; Freitas, R.d.A. Immunohistochemical evaluation of the inflammatory response in periodontal disease. *Braz. Dent. J.* **2008**, *19*, 9–14. [CrossRef]
30. Loos, B.G.; Van Dyke, T.E. The role of inflammation and genetics in periodontal disease. *Periodontol. 2000* **2020**, *83*, 26–39. [CrossRef] [PubMed]
31. Cekici, A.; Kantarci, A.; Hasturk, H.; Van Dyke, T.E. Inflammatory and immune pathways in the pathogenesis of periodontal disease. *Periodontol. 2000* **2014**, *64*, 57–80. [CrossRef] [PubMed]
32. Loesche, W.J.; Gusberti, F.; Mettraux, G.; Higgins, T.; Syed, S. Relationship between oxygen tension and subgingival bacterial flora in untreated human periodontal pockets. *Infect. Immun.* **1983**, *42*, 659–667. [CrossRef] [PubMed]
33. Schroeder, H.E.; Listgarten, M.A. The gingival tissues: The architecture of periodontal protection. *Periodontol. 2000* **1997**, *13*, 91–120. [CrossRef] [PubMed]
34. Le, N.; Cheng, H.; Subhash, H.; Kilpatrick-Liverman, L.; Wang, R.K. Gingivitis resolution followed by optical coherence tomography and fluorescence imaging: A case study. *J. Biophotonics* **2021**, *14*, e202100191. [CrossRef]
35. Șurlin, P.; Camen, A.; Stratul, S.I.; Roman, A.; Gheorghe, D.N.; Herăscu, E.; Osiac, E.; Rogoveanu, I. Optical coherence tomography assessment of gingival epithelium inflammatory status in periodontal—Systemic affected patients. *Ann. Anat.* **2018**, *219*, 51–56. [CrossRef]
36. Fernandes, L.O.; Mota, C.C.B.O.; Oliveira, H.O.; Neves, J.K.; Santiago, L.M.; Gomes, A.S.L. Optical coherence tomography follow-up of patients treated from periodontal disease. *J. Biophotonics* **2019**, *12*, e201800209. [CrossRef] [PubMed]
37. Fischer, K.R.; Büchel, J.; Testori, T.; Rasperini, G.; Attin, T.; Schmidlin, P. Gingival phenotype assessment methods and classifications revisited: A preclinical study. *Clin. Oral Investig.* **2021**, *25*, 5513–5518. [CrossRef]
38. Liu, K.; Zhu, T.; Gao, M.; Yin, X.; Zheng, R.; Yan, Y.; Gao, L.; Ding, Z.; Ye, J.; Li, P. Functional OCT angiography reveals early retinal neurovascular dysfunction in diabetes with capillary resolution. *Biomed. Opt. Express* **2023**, *14*, 1670–1684. [CrossRef] [PubMed]
39. Kashani, A.H.; Chen, C.L.; Gahm, J.K.; Zheng, F.; Richter, G.M.; Rosenfeld, P.J.; Shi, Y.; Wang, R.K. Optical coherence tomography angiography: A comprehensive review of current methods and clinical applications. *Prog. Retin. Eye Res.* **2017**, *60*, 66–100.
40. Park, J.Y.; Chung, J.H.; Lee, J.S.; Kim, H.J.; Choi, S.H.; Jung, U.W. Comparisons of the diagnostic accuracies of optical coherence tomography, micro-computed tomography, and histology in periodontal disease: An ex vivo study. *J. Periodontal Implant. Sci.* **2017**, *47*, 30–40. [CrossRef]
41. Otis, L.L.; Colston, B.W.; Everett, M.J., Jr.; Nathel, H. Dental optical coherence tomography: A comparison of two in vitro systems. *Dentomaxillofac. Radiol.* **2000**, *29*, 85–90. [CrossRef]